JMEPEG (2016) 25:4764–4768
DOI: 10.1007/s11665-016-2348-1

1059-9495/$19.00

The Microstructure and Thermoelectric Properties of Yb-Filled Skutterudite $Yb_{0.1}Co_4Sb_{12}$ Under Cyclic Thermal Loading

Pengfei Wen, Yan Zhu, Jihu Chen, Houjiang Yang, and Pengcheng Zhai

(Submitted March 30, 2016; in revised form September 10, 2016; published online September 28, 2016)

This paper is devoted to investigating the microstructure and thermoelectric properties of Yb-filled skutterudite $Yb_{0.1}Co_4Sb_{12}$ under a cyclic thermal loading from room temperature to 773 K. The results indicate after 1000 cycles, the surface morphology changes dramatically, and clear grain boundaries appear on the surface of the sample. The grain sizes of the sample change little after 1000 cycles, and the main phase is still skutterudite; however, a trace amount of YbSb also exists. In addition, the electrical conductivity and thermal conductivity decrease distinctly after 1000 cycles, but the absolute value of the Seebeck coefficient increases a little. Consequently, the *ZT* value decreases slightly from 0.75 at 800 K before cycling to 0.69 after 1000 cycles. It indicates that the effect of the cyclic thermal loading on the *ZT* of the $Yb_{0.1}Co_4Sb_{12}$ material is not distinct.

Keywords cyclic thermal loading, skutterudite, structure, thermoelectric properties

1. Introduction

Thermoelectric (TE) conversion has received worldwide attention for the applications in electric cooling, waste heat recovery, and power generation (Ref 1-3). The conversion efficiency and the reliability of TE devices are two major concerns in their practical applications. The conversion efficiency of TE devices is greatly related to the dimensionless figure of merit, $ZT = (\alpha^2\sigma/\kappa)T$, where α, σ, κ, and T are the Seebeck coefficient, electrical conductivity, thermal conductivity, and absolute temperature, respectively. In addition, once the TE material of a device is selected, the reliability of the TE material during serving time becomes another important issue.

Skutterudite compounds have attracted much attention in the last decade as promising TE materials. One of the remarkable features of skutterudites is that the guest atoms can be introduced into their cage-like framework structure to form the filled skutterudites, which are suggested as ''phonon glass/electron crystal'' materials (Ref 4). The ''rattling'' motion of the filled atoms can effectively scatter phonons and cause a significant decrease in the lattice thermal conductivity. The rare earths (Ref 5-7), alkali earths (Ref 8), and alkaline earths (Ref 9, 10) are often used as fillers, such as Yb, La, Ce, Ba, Eu. Of the filler species above, Yb is considered as one of the most effective fillers to get the lowest thermal conductivity (Ref 11-16). Therefore, Yb-filled skutterudite TE material is considered as one of the most suitable materials in the power generation system. However, it is worth noticing that the evolution of structure and thermal properties of Yb-filled skutterudite under serving conditions has been scantily studied so far.

In addition, it is generally known that when TE materials are used for solar-electrical energy generation, the materials will inevitably suffer cyclic thermal loading, because of diurnal variation. Therefore, it is essential to evaluate the reliability of TE materials under cyclic thermal loading. However, continuous thermal load is usually selected as the thermal loading to study the reliability of TE materials because it is easier to implement. Zhao et al. (Ref 17) have studied the sublimation of Sb in $CoSb_3$ by a thermal duration test. In our earlier work, we have investigated the effects of thermal annealing on the microstructure and thermoelectric properties of nano-TiN/$Co_4Sb_{11.5}Te_{0.5}$ composites (Ref 18) and nanostructured $CoSb_3$ (Ref 19).

In this study, we report on the evolution of the microstructures and thermoelectric properties of Yb-filled skutterudite $Yb_{0.1}Co_4Sb_{12}$ under cyclic thermal loading. As the highest working temperature of the skutterudite-based TE device is about 773 K, the thermal cycling experiment from room temperature to 773 K was designed to simulate the service condition.

2. Experiment

2.1 Thermal Cycling Experiment

Highly pure metals of Yb (99.999%, shot), Co (99.99%, shot), and Sb(99.9999%, shot)were used as starting materials. The constituent elements were weighed according to the $Yb_{0.1}Co_4Sb_{12}$ formula and then loaded into a carbon-coated silica tube. The tube was then sealed under a pressure of 10^{-3} Pa. The silica ampoule was heated to 1273 K at rate of 2 K/min and kept at 1273 K for 24 h. After that the silica

Pengfei Wen, Yan Zhu, Jihu Chen, Houjiang Yang, and **Pengcheng Zhai**, Department of Engineering Structure and Mechanics, Wuhan University of Technology, Wuhan Hubei, China; and **Yan Zhu**, Department of Civil and Architectural Engineering, Wuhan Huaxia University of Technology, Wuhan, Hubei, China. Contact e-mail: pczhai@126.com and pfwen@126.com.

ampoule was quenched in a water bath. The obtained ingots were ground into fine powder and pressed into cylindrical pellets. The pellets were sealed in a silica tube again and annealed at 948 K for 168 h to form a completely homogeneous crystallographic phase. The reacted materials were milled into fine powder and sintered by spark plasma sintering (SPS) under 40 MPa at 903 K for 7 min. As-prepared samples of different sizes (e.g., $3 \times 3 \times 10$ mm^3 and $8 \times 8 \times 1.5$ mm^3 for measurement of electrical properties and thermal properties, respectively) were cut from the sintered bulk material. After the characterization of the microstructures and TE properties of the as-prepared samples was finished, these as-prepared samples were sealed into vacuum quartz tubes. The tubes were held at 773 K for 10 min in a constant temperature furnace. Then, the tubes were taken out to cool down to room temperature. After each five hundred cycles of each tube, the microstructures and TE properties of the samples were characterized.

2.2 Measurement Methods

The microstructure was characterized by means of scanning electron microscopy (SEM). The phase was characterized by powder x-ray diffractometry (XRD). The density d was measured by the Archimedes method. The electrical conductivity (σ) and the Seebeck coefficient (α) were measured synchronously by the standard four-probe method (Sinkuriko, ZEM-1) in Ar atmosphere. The thermal conductivity (κ) was calculated from the measured thermal diffusivity D, the specific heat Cp, and the density d by the relationship $\kappa = DC_pd$, where D and C_p were measured by a laser flash method (Sinkuriko, TC-7000) in vacuum. The σ, α, D, and C_p were measured in the temperature range of 300–800 K.

3. Results and Discussion

3.1 Structures

Figure 1 displays the cross section of the $Yb_{0.1}Co_4Sb_{12}$ bulk material after different thermal cycles. As can be seen, the grain sizes of sample change little after 1000 cycles. It indicates that the grain sizes of the $Yb_{0.1}Co_4Sb_{12}$ bulk materials are stable under the cyclic thermal loading. However, the surface morphology changes dramatically as shown in Fig. 2. Before thermal cycling, the sample's surface is smooth. However, after 1000 cycles, clear grain boundaries appear, as shown in Fig. 2(b). The change on surface morphology is due to the volatilization of Sb (Ref 17, 20). The volatilization of Sb results in the higher surface tension on the sample. When the surface tension force reaches a critical value, cracks appear on the sample's surface (Ref 17).

Figure 3 shows x-ray diffraction patterns of the sample after different cycles. It can be seen that the sample is composed of a single-phase compound with a skutterudite structure before cycling. After 1000 cycles, the major phase in the sample is still skutterudite; however, a weak peak is observed in the x-ray pattern of the sample, which is attributed to the characteristic diffraction peak of YbSb. In addition, no evident peak shift for the characteristic diffraction peaks of skutterudite is observed in the x-ray pattern of the sample after thermal cycling, implying that no serious strain exists in the sample after 1000 cycles. The densities of the sample after different cycles are shown in Table 1. After 1000 cycles, the density decreases by 3.3%. It is attributed to the volatilization of Sb, which will lead to the decrease in the sample's mass and the increase in the sample's volume.

3.2 TE Properties

The temperature dependence of the electrical conductivity for $Yb_{0.1}Co_4Sb_{12}$ after different cycles is shown in Fig. 4(a). As can be seen, the electrical conductivity of the sample decreases with increasing temperature, which indicates a metallic transport behavior. The decline in the electrical conductivity with increasing temperature mainly originates from the enhancement in the scattering effect of the carriers on the crystal lattice. After thermal cycling, the electrical conductivity decreases obviously. The value of the electrical conductivity at 300 K decreases by 15.5% after 1000 cycles, compared with that before cycling. The reduction in the electrical conductivity with increasing thermal cycles may be due to the following reasons. Firstly, the reduction in the electrical conductivity may be attributed to the higher porosity, and the relationship between the electrical conductivity and the relative density can be described as (Ref 21):

$$\sigma = \frac{(3C-1)}{2}\sigma_{\mathrm{f}} \qquad \text{(Eq 1)}$$

where C is the relative density and σ_{f} is the theoretic electrical conductivity. Secondly, the sublimation of Sb will give

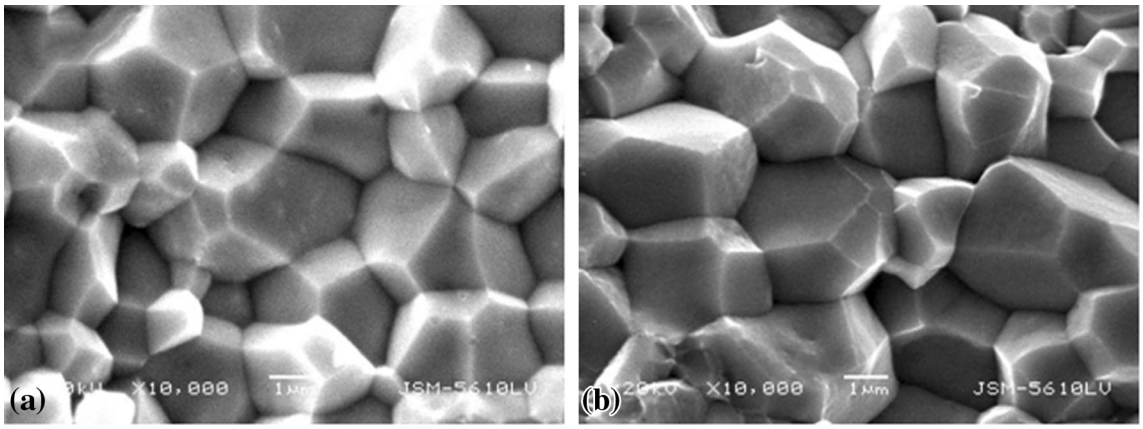

Fig. 1 SEM images of the cross section of the sample at different cycles (a) before cycling and (b) 1000 cycles

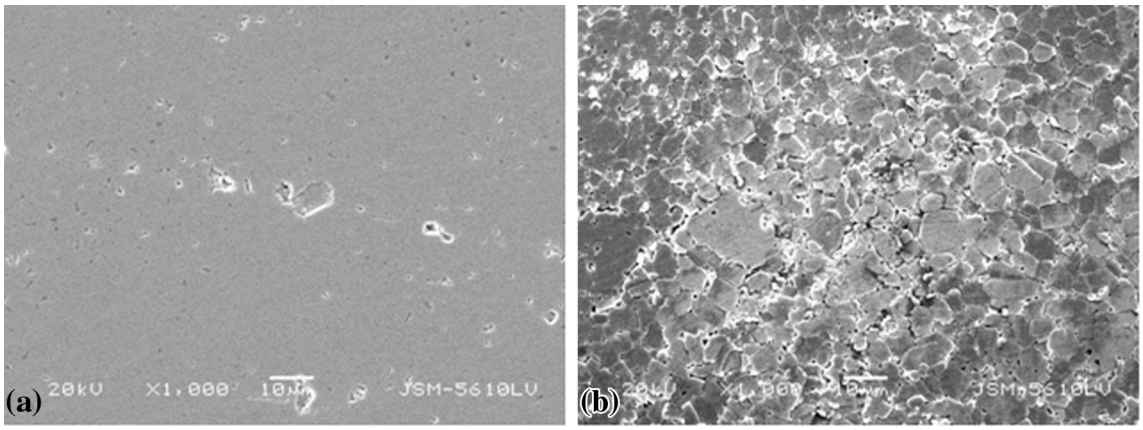

Fig. 2 SEM images of the sample's surface at different cycles (a) before cycling and (b) 1000 cycles

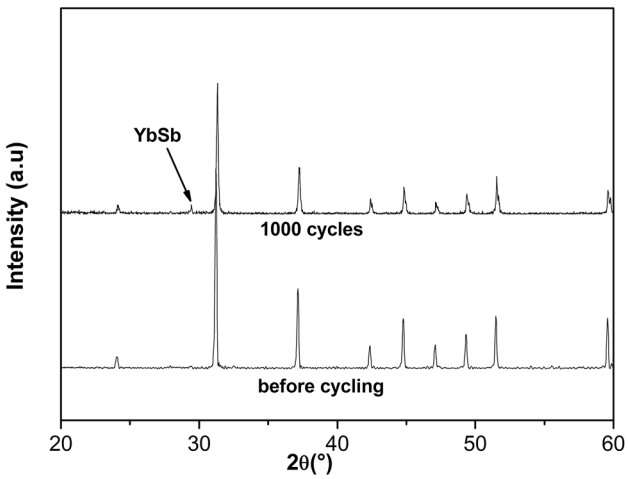

Fig. 3 X-ray diffraction patterns of the sample at different cycles

Table 1 Density and relative density of the sample at different cycles

Cycle time	0	500	1000
Density (g/cm^3)	7.45	7.36	7.2
Relative density (%)	98	96	94

birth to the decrease in the carrier concentration of n-type skutterudite, which also may result in the decline of the electrical conductivity (Ref 17). Additionally, secondary precipitates may enhance the scattering effect of the carriers (Ref 22).

The temperature dependence of the Seebeck coefficient for $Yb_{0.1}Co_4Sb_{12}$ after different cycles is shown in Fig. 4(b). The sample shows n-type conduction with negative Seebeck coefficient. The absolute value of the sample's Seebeck coefficient increases after thermal cycling compared to that before cycling. The $|\alpha|$ of 143.7 μVK^{-1} for the sample at 300 K before cycling increases to 150 μVK^{-1} for the sample after 1000 cycles. The increase in the Seebeck coefficient is originated from the decrease in the carrier concentration (Ref 17) and the secondary precipitates (Ref 22). The higher porosity plays little role on the Seebeck coefficient. The effective Seebeck coefficient of a two-phase composite can be expressed as (Ref 23):

$$\alpha = \frac{6\kappa\langle\alpha_i D_i\rangle}{1 - 3\langle\kappa_i D_i\rangle} \quad \text{(Eq 2)}$$

with:

$$D_i = \frac{\sigma_i}{(\kappa_i + 2\kappa)(\sigma_i + 2\sigma)} \quad \text{(Eq 3)}$$

where κ and σ are the effective thermal conductivity and the electrical conductivity, respectively, which are given as follows:

$$\left\langle \frac{\kappa_i - \kappa}{\kappa_i + 2\kappa} \right\rangle = 0 \quad \text{(Eq 4)}$$

$$\left\langle \frac{\sigma_i - \sigma}{\sigma_i + 2\sigma} \right\rangle = 0 \quad \text{(Eq 5)}$$

where the subscript i denotes the i-th phase and $\langle\ \rangle$ denotes the volume average. For the porous phase, its thermal and electrical conductivities can be taken as zero. Therefore, from Eq 2, it can be concluded that the Seebeck coefficient of the sample will not change because of the higher porosity.

The temperature dependence of the thermal conductivity for $Yb_{0.1}Co_4Sb_{12}$ after different cycles is shown in Fig. 4(c). The lattice thermal conductivity κ_L is obtained by subtracting the electronic component κ_C ($\kappa_C = L\sigma T$, where L is Lorenz constant, $L = 2.45 \times 10^{-8}$ V^2 K^{-2}) (Ref 24) from the total thermal conductivity κ. It can be concluded that the thermal conductivity of the sample is mainly attributed to the lattice contribution, as shown in Fig. 4(c). The κ of 4.14 Wm^{-1} K^{-1} at 300 K for the sample before cycling decreases to 3.71 Wm^{-1} K^{-1} for the sample after 1000 cycles. On the one hand, it is attributed to the enhancement of phonon scattering induced by the secondary precipitates on the grain boundaries (Ref 22). On the other hand, the higher porosity may lead to the lower thermal conductivity, which can be interpreted by the Maxwell-Eucken equation (Ref 25):

$$\kappa = \kappa_0 \frac{1 - p}{1 + \beta p} \quad \text{(Eq 6)}$$

where p is the porosity, κ_0 is the bulk conductivity, and β is a constant determined by the conditions of the pores.

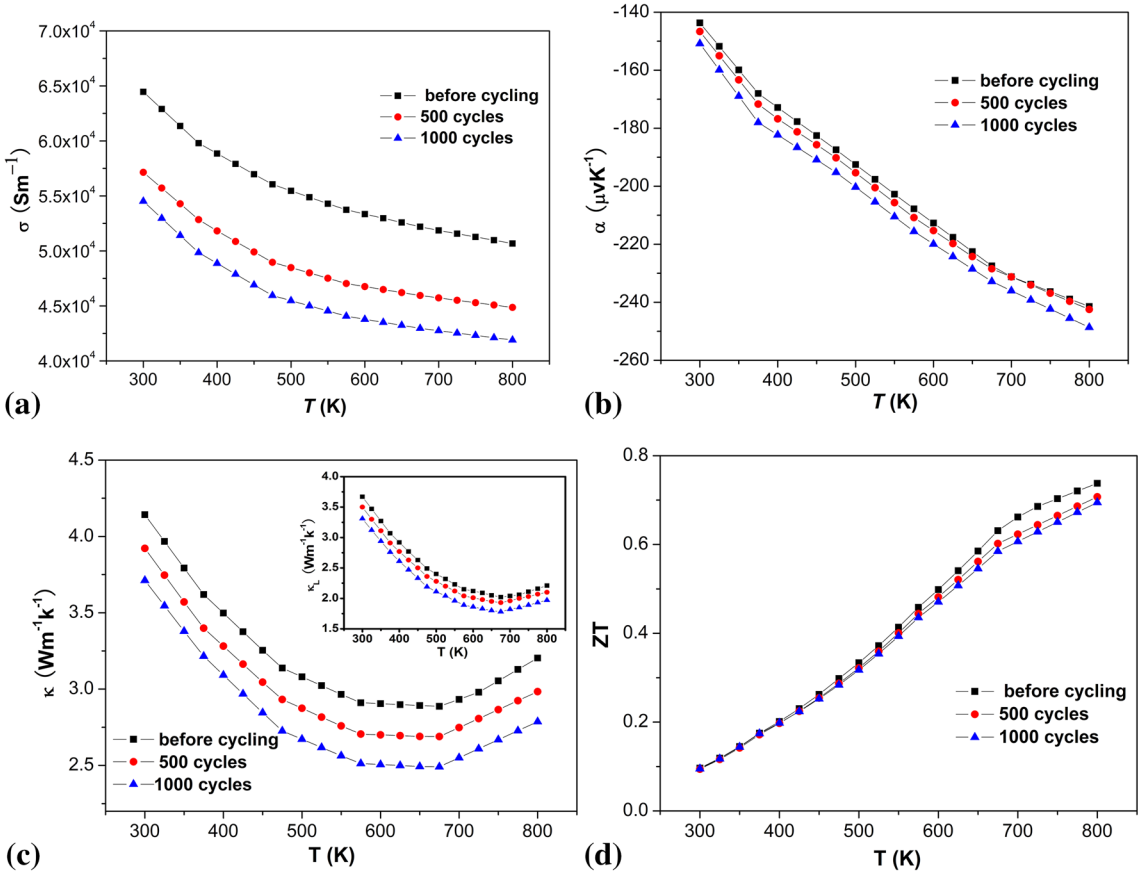

Fig. 4 Temperature dependence of (a) the electrical conductivity, (b) the Seebeck coefficient, (c) the thermal conductivity and lattice thermal conductivity (inset), and (d) the ZT value for $Yb_{0.1}Co_4Sb_{12}$ at different cycles

The temperature dependence of the *ZT* value for $Yb_{0.1}Co_4Sb_{12}$ after different cycles is shown in Fig. 4(d). Compared with before cycling, the change in the *ZT* value is not distinct. The *ZT* of 0.75 at 800 K for the sample before cycling slightly decreases to 0.69 after 1000 cycles. It indicates that the effect of the cyclic thermal loading on the *ZT* of the $Yb_{0.1}Co_4Sb_{12}$ material is not distinct.

4. Conclusion

In this study, we report on the evolution of the microstructures and thermoelectric properties of Yb-filled skutterudite $Yb_{0.1}Co_4Sb_{12}$ under cyclic thermal loading from room temperature to 773 K. Under cyclic thermal loadings, the grain sizes of sample change little, but the surface morphology changes dramatically, and clear grain boundaries appear. In addition, the density decreases by 3.3% after 1000 cycles. The electrical conductivity and the thermal conductivity decrease obviously compared with those before cycling. However, the absolute value of Seebeck coefficient increases slightly. The *ZT* value decreases slightly from 0.75 at 800 K before cycling to 0.69 after 1000 cycles. It indicates that the effect of the cyclic thermal loading on the *ZT* of the $Yb_{0.1}Co_4Sb_{12}$ material is not distinct.

Acknowledgments

This study is supported by the National Natural Science Foundation of China (11402182 and 11502182), the 973 Program (2013CB632505), and the Fundamental Research Funds for the Central Universities (WUT: 2014-Ia-023, 2015IA013).

References

1. L.E. Bell, Cooling, Heating, Generating Power and Recovering Waste Heat with Thermoelectric Systems, *Science*, 2008, **321**, p 1457–1461
2. M.S. Dresselha, G. Chen, M.Y. Tang, R.G. Yang, H. Lee, D.Z. Wang, Z.F. Ren, J.P. Fleurial, and P. Gogna, New Directions for Low-Dimensional Thermoelectric Materials, *Adv. Mater.*, 2007, **19**, p 1043–1053
3. H. Scherrer, L. Vikhor, B. Lenoir, A. Dauscher, and P. Poinas, Solar Thermolectric Generator Based on Skutterudites, *J. Power Sources*, 2003, **115**, p 141–148
4. G.S. Nolas, D.T. Morelli, T.M. Tritt, SKUTTERUDITES: A Phonon-Glass-Electron Crystal Approach to Advanced Thermoelectric Energy Conversion Applications, *Annu. Rev. Mater. Sci.*, 1999, **29**, p 89–116
5. V.L. Kuznetsov, L.A. Kuznetsov, and D.M. Rowe, Effect of Partial Void Filling on the Transport Properties of $Nd_xCo_4Sb_{12}$ Skutterudites, *J. Phys. Condens. Matter.*, 2003, **15**, p 5035–5048
6. G.A. Lamberton, Jr., S. Bhattacharya, R.T. Littleton, IV, M.A. Kaeser, R.H. Tedstrom, T.M. Tritt, J. Yang, and G.S. Nolas, High Figure of Merit in Eu-Filled $CoSb_3$-Based Skutterudites, *Appl. Phys. Lett.*, 2002, **80**, p 598–600
7. J. Yang, D.T. Morelli, G.P. Meisner, W. Chen, J.S. Dyck, and C. Uher, Effect of Sn Substituting for Sb on the Low-Temperature Transport Properties of Ytterbium-Filled Skutterudite, *Phys. Rev. B*, 2003, **67**, p 165207-1-6
8. Y.Z. Pei, L.D. Chen, W. Zhang, X. Shi, S.Q. Bai, X.Y. Zhao, Z.G. Mei, and X.Y. Li, Synthesis and Thermoelectric Properties of $K_yCo_4Sb_{12}$, *Appl. Phys. Lett.*, 2006, **89**, p 221107-1-3
9. L.D. Chen, T. Kawahara, X.F. Tang, T. Goto, T. Hirai, J.S. Dyck, W. Chen, and C. Uher, Anomalous Barium Filling Fraction and n-Type

Thermoelectric Performance of $Ba_yCo_4Sb_{12}$, *J. Appl. Phys.*, 2001, **90**, p 1864–1868

10. M. Puyet, B. Lenoir, A. Dauscher, P. Pécheur, C. Bellouard, J. Tobola, and J. Hejtmanek, Electronic, Transport, and Magnetic Properties of $Ca_xCo_4Sb_{12}$ Partially Filled Skutterudites, *Phys. Rev. B*, 2006, **73**, p 035126-1-12
11. G.S. Nolas, M. Kaeser, R.T. Littleton, IV, and T.M. Tritt, High Figure of Merit in Partially Filled Ytterbium Skutterudite Materials, *Appl. Phys. Lett.*, 2000, **77**, p 1855–1857
12. Jiro. Nagao, Devaraj. Nataraj, Marhoun. Ferhat, Tsutomu. Uchida, Satoshi. Takeya, Takao. Ebinuma, Hiroaki. Anno, Kakuei. Matsubara, Eiji. Hatta, and Koichi. Mukasa, Phonon Behaviors and Electronic Structures of the Filled Skutterudite $Yb_yCo_4Sb_{12}$ Compounds: An Electron Tunneling Study, *J. Appl. Phys.*, 2002, **92**, p 4135–4137
13. N.R. Dilley, E.D. Bauer, M.B. Maple, and B.C. Sales, Thermoelectric Properties of Chemically Substituted Skutterudites $Yb_yCo_4Sn_xSb_{12-x}$, *J. Appl. Phys.*, 2000, **88**, p 1948–1951
14. X. Shi, W. Zhang, L.D. Chen, and J. Yang, Filling Fraction Limit for Intrinsic Voids in Crystals: Doping in Skutterudites, *Phys. Rev. Lett.*, 2005, **95**, p 185503-1-4
15. X. Shi, W. Zhang, L.D. Chen, J. Yang, and C. Uher, Theoretical Study of the Filling Fraction Limits for Impurities in $CoSb_3$, *Phys. Rev. B*, 2006, **75**, p 235208-1-8
16. X. Shi, H. Kong, C.-P. Li, C. Uher, J. Yang, J.R. Salvador, H. Wang, L. Chen, and W. Zhang, Low Thermal Conductivity and High Thermoelectric Figure of Merit in n-Type $Ba_xYb_yCo_4Sb_{12}$ Double-Filled Skutterudites, *Appl. Phys. Lett.*, 2008, **92**, p 182101-1-3
17. D.G. Zhao, C.W. Tian, Y.T. Liu, C.W. Zhan, and L.D. Chen, High Temperature Sublimation Behavior of Antimony in $CoSb_3$ Thermoelectric Material During Thermal Duration Test, *J. Alloys Comp.*, 2011, **509**, p 3166–3171
18. P.F. Wen, B. Duan, P.C. Zhai, P. Li, and Q.J. Zhang, Effect of Thermal Annealing on the Microstructure and Thermoelectric Properties of Nano-TiN/$Co_4Sb_{11.5}Te_{0.5}$ Composites, *J. Mater. Sci. Mater. Electron.*, 2013, **24**, p 5155–5161
19. P.F. Wen, P. Li, Q.J. Zhang, Z.W. Ruan, L.S. Liu, and P.C. Zhai, Effects of Annealing on Microstructure and Thermoelectric Properties of Nanostructured $CoSb_3$, *J. Electron. Mater.*, 2013, **42**, p 1443–1448
20. P.F. Wen, P. Li, Q.J. Zhang, F.J. Yi, L.S. Liu, and P.C. Zhai, Effect of Cyclic Thermal Loading on the Microstructure and Thermoelectric Properties of $CoSb_3$, *J. Electron. Mater.*, 2009, **38**, p 1200–1205
21. R. Landauer, The Electrical Resistance of Binary Metallic Mixtures, *J. Appl. Phys.*, 1952, **3**, p 779–784
22. P. Wei, W.Y. Zhao, C.L. Dong, X. Yang, J. Yu, and Q.J. Zhang, Excellent Performance Stability of Ba and In Double-Filled Skutterudite Thermoelectric Materials, *Acta Mater.*, 2011, **59**, p 3244–3254
23. I. Webmam, J. Jortner, and M.H. Cohen, Thermoelectric Power in Inhomogeneous Materials, *Phys. Rev. B.*, 1977, **16**, p 2959–2964
24. M.S. Toprak, C. Stiewe, D. Platzek, S. Williams, L. Bertini, E. Müller, C. Gatti, Y. Zhang, M. Rowe, and M. Muhammed, the impact of nanostructuring on the Thermal Conductivity of Thermoelectric $CoSb_3$, *Adv. Funct. Mater.*, 2004, **14**, p 1189–1196
25. J. Adachi, K. Kurosaki, M. Uno, and S. Yamanaka, Effect of Porosity on Thermal and Electrical Properties of Polycrystalline Bulk ZrN Prepared by Spark Plasma Sintering, *J. Alloys Comp.*, 2007, **432**, p 7–10